

Fabrication and characterization copper/diamond composites for heat sink application using powder metallurgy

Zeinab Abdel Hamid^{1*}, Sayed F. Moustafa¹, Fatma A. Morsy², Nevien Abdel Atty Khalifa², Fatma Abdel Mouez¹

¹Central Metallurgical R & D Institute, CMRDI, Cairo, Egypt; *Corresponding Author: forzeinab@yahoo.com

²Faculty of Science, Chemistry department, Helwan University, Helwan, Egypt.

Received 27 July 2011; revised 30 August 2011; accepted 10 September 2011.

ABSTRACT

Copper composites reinforced with diamond particles were fabricated by the powder metallurgical technique. Copper matrix and diamond powders were mixed mechanically, cold compacted at 100 bar then sintered at 900°C. The prepared powders and sintered copper/diamond composites were investigated using X-ray diffraction (XRD) and scanning electron microscope equipped with an energy dispersive X-ray analysis (SEM/EDS). The effect of diamond contents in the Cu/diamond composite on the different properties of the composite was studied. On fracture surfaces of the Cu/uncoated diamond composites, it was found that there is a very weak bonding between diamonds and pure copper matrix. In order to improve the bonding strength between copper and the reinforcement, diamond particles were electroless coated with NiWB alloy. The results show that coated diamond particles distribute uniformly in copper composite and the interface between diamond particles and Cu matrix is clear and well bonded due to the formation of a thin layer from WB₂, Ni₃B, and BC₂ between Cu and diamond interfaces. The properties of the composites materials using coated powder, such as hardness, transverse rupture strength, thermal conductivity, and coefficient of thermal expansion (CTE) were exhibit greater values than that of the composites using uncoated diamond powder. Additionally, the results reveals that the maximum diamond incorporation was attained at 20 V_f%. Actually, Cu/20 V_f% coated diamond composite yields a high thermal conductivity of 430 W/mK along with a low coefficient of thermal expansion (CTE) $6 \times 10^{-6}/K$.

Keywords: Powder Metallurgy; Ceramic-Matrix Composites (CMCs); Ceramics; Coating; Electroless

1. INTRODUCTION

In order to dissipate the heat generated in electronic packages effectively, suitable materials must be selected as heat spreaders and heat sink [1-6]. The ideal material working as heat sink and heat spreader should have a low coefficient of thermal expansion (CTE) and a high thermal conductivity. Copper as it has the highest thermal conductivities in metal, has been used for decades as the material of choice as heat sink for semiconductor electronic packages. Unfortunately, copper has become a bottleneck in removing heat from semiconductor devices, and its thermal conductivity becomes not enough to dissipate the heat generated from the new generation of semiconductor components. In addition to bulk thermal conductivity which must be removed, thermal expansion coefficients of semiconductors of silicon or gallium arsenide are low compared to other materials and much smaller than that of copper which is usually used as a heat sink for semiconductors. The differences in coefficient of thermal expansion properties leads to formation of stresses, which can lead to the component becoming distorted, detached or even fractured. Stresses may form during production of the semiconductor chip, specifically during the cooling phase from the soldering temperature to room temperature. However, temperature fluctuations also occur when the package is operating, ranging from -50°C to 200°C, which can lead to thermo-mechanical stresses. As copper and other metals exhibit thermal expansion rates that are an order of magnitude greater than those of silicon and gallium arsenide, it is problematic to attach these metals to semiconductor chips. In fact, many packaging solutions sacrifice on

thermal conductivity, choosing less efficient heat conductors such as ceramics in order to address this issue [6].

There is a great demand for a new material to be used as heat sink substrate. This new material should have high thermal conductivity greater than that of copper (*i.e.* as great as possible) in order to dissipate the high heat generated from the semiconductor component during operation, and in the same time its coefficient of thermal expansion must match as closely as possible to that of the semiconductor component. This new material could be developed by means of composite materials such as Cu/diamond composite. Since diamond is characterized by high thermal conductivity about 6 times that of copper but its disadvantage that its thermal expansion is smaller than that of semiconductors. So by adding copper to diamond we can have the required characteristics by controlling the percentages of copper to diamond [7-9]. The major problems encountered with "diamond on copper" synthesis are the low nucleation density, film cracking, and poor wettability. When diamond particles are embedded in a copper matrix, the interface plays a crucial role in determining the thermal conductivity, the CTE and also the mechanical properties of the composite. An ideal interface should provide good adhesion and minimum thermal boundary resistance.

It is well known that alloying of copper with a strong carbide diamond forming element promotes wetting and bonding of diamond. Even in the case of solid phase bonding (e.g. hot pressing), high bonding strength was observed for copper alloys with minor additions of carbides from (Ti, Cr, B or Zr) [10,11]. Chromium or tungsten is believed to be a good promoter due to its abilities to inhibit bulk copper formation, to improve copper thermal stability and to increase copper dispersion. The main objective of this investigation is to synthesize and characterize Cu/diamond composite materials for electronic application obtained by powder metallurgy technique. Coating diamond particles using electroless technique added to the copper matrix to fabricate Cu/diamond composite has been investigated. Finally, the properties of Cu/coated diamond composites were compared with the same materials containing uncoated diamond.

2. EXPERIMENTAL PROCEDURES

2.1. General

In the present work, the fabrication of Cu/diamond composites using powder metallurgy technique was investigated in detail. The investigated diamond powders of micron grain sizes (20 - 40 μm) type RVD were supplied by Polaris Diamond Powder Co., Ltd. The diamond powder was electroless coated with NiWB. Cop-

per powder using in this study has been fabricated using electroless technique.

2.2. Surface Treatment for Diamond and Electroless NiWB Plating

As the diamond surface has higher interface energy, the adhesion of surface with the coating layer is bad, and it makes the diamond shatter easily. For solving this, the diamond surface must be treated and activated to improve the coating adhesion. The following steps were used for surface treatment.

Washing by acetone (30 min.); etching by acidic solution using 50% HNO_3 ; sensitization using stannous chloride solution; activation using palladium chloride solution; then immersed in the plating solution [12].

The diamond after sensitization and activation were chemically coated with NiWB. The chemical composition and the operating conditions of the plating solution were illustrated in **Table 1**. Additionally, the chemical composition and the operating conditions for producing the copper powder using electroless technique were illustrated in **Table 2**. Analytical reagents and distilled water were used to prepare the plating solutions.

Table 1. Chemical composition and operating conditions of electroless NiWB plating solution.

Composition	Concentration, g^{-1} NiWB
Nickel sulphate	10
sodium citrate	20
Dimethyl amine borane (DMAB)	0.4
sodium Tungstate	20
Operating conditions	
Temperature, $^{\circ}\text{C}$	85
pH	6.5
Time, hrs	2

Table 2. The chemical composition and the operating conditions of electroless copper solution.

Composition	Concentration g^{-1}
Copper sulphate	35
Sodium potassium tartrate	170
Sodium hydroxide	50
Formaline	200 mL^{-1}
Operating conditions	
pH	11 - 13
Temperature, $^{\circ}\text{C}$	25

2.3. Composites Production

The amount of powder and coating thickness must be controlled during the production of composite. If a too large amount of diamond or a too thick coating for the functional layer is used the thermal conductivity of the copper matrix material will be reduced very severe. The copper powders were mixed with the diamond particles to prepare composites then milled for 20 min, compacted under the pressure 100 bar then sintered at 900°C for 1 hr using hydrogen atmosphere.

2.4. Analysis and Characterizations

Scanning electron microscope (SEM) with a link energy dispersive X-ray spectroscopy (EDS) detector attachment, model JEOL, JSM-5410, were used to assess the surface morphology, particle size, particle shape, agglomeration of particles and the compositions of the various Cu/diamond composites. For SEM, the dry powder was dusted onto a carbon tape, which was stuck onto the copper holder disk of the microscope, gently blown with compressed air before introducing into the microscope chamber.

The phase identification was determined using X-ray diffraction PANalytical X'pert PRO (45 kv/40 mA) advanced with Cu target ($\lambda = 1.54 \text{ \AA}$). The boron content of the NiWB thin film deposited was determined by inductively coupled plasma-mass spectrometer (ICP-MS) after dissolving the deposited layer in nitric acid solution.

2.5. The Densities Measurements

The densities of the sintered powders were measured according to MPIF Standards 42, 1998, using Archimedes rule. The density (δ) of the samples was calculated according to the following formula [13,14]:

$$\delta = W_a / (W_a - W_w) \quad \text{gm/cm}^3 \quad (1)$$

where W_a and W_w are the weights in air and water respectively.

2.6. The Electrical Resistivity Measurements

The electrical resistivity of the sintered materials was measured using the four-probe method by using Omega CL 8400 micrometer device. The rectangular sintered specimen was placed in a specially designed jig for making the electrical connection. Measurements were taken for the longitudinal and the transverse directions of the sample. The resistivity (ρ) was calculated according to the following equation by using High Precision Microhmeter.

$$\rho = (R \cdot A) / L \quad (2)$$

where, R is the resistance in micro ohm, L is the measured length in cm, A is the cross section area in cm^2 , and ρ is the resistivity in $\mu\Omega \cdot \text{cm}$.

2.7. The Macrohardness Measurements

The macrohardness values of the investigated materials were measured as the average of 5 readings over the surface of the specimens using Vicker's macrohardness Test type HPV 30 A and the using load was 5 kg for 15 s.

2.8. Transverse Rupture Strength (TRS) Measurements

The rupture test was performed using compression testing machine and a test fixture, according to MPIF Standard 41. All the samples of the powders were compacted into rectangular compacts of dimension of $(30 \times 10 \times 6) \text{ mm}^3$. In the transverse rupture fixture, the test bar was placed centrally located and perpendicular to the supporting rods with the top up. The fixture with the test bar was placed between the plates of the compression testing machine and the load was applied at constant rate of 2.5 mm/min, until the test bar fractured. The transverse rupture strength for sintered samples was calculated according to the following expression [13]:

$$TRS = \frac{3PL}{2t^2W} \quad (3)$$

where: TRS = Transverse rupture strength in N/mm^2

P = Fracturing (rupture) load (N)

L = the distance between the supporting rods (25.4 mm)

t = the thickness of the sample in (mm)

W = the width of the sample in (mm)

2.9. Coefficient of Thermal Expansion (CTE)

CTE was measured with a Netzsch dilatometer model 402 C push rod. The samples were tested in open air between 25°C and 160°C at a heating rate of 3 K/min. Further on, the reproducibility was checked by measuring the same sample twice. The system was calibrated with a copper standard prior to the sample test run. Coefficient of thermal expansion (CTE) value at a given temperature was calculated from the thermal expansion curves (change in length versus temperature) recorded during heating up the specimen from room temperature up to 160°C, according to this relationship:

$$CTE = \frac{\partial}{\partial T} \left(\frac{\Delta L}{L} \right) \quad (4)$$

where L represents the original length of the specimen

and ΔL stands for the length change after a thermal cycling.

2.10. Thermal Conductivity

The thermal conductivity was calculated from electrical resistivity measurement using Wiedemann and Franz equation which derived a relation equation between the thermal and electrical conductivities [15]. The Wiedemann-Franz equation is as follows:

$$\frac{\lambda}{\sigma T} = \frac{\pi^2 k_B^2}{3e^2} = L = 2.443 \times 10^{-8} \text{ J}\Omega/\text{K}^2\text{s} \quad (5)$$

where, λ is thermal conductivity (W/mK), σ is electrical conductivity $\mu\Omega\cdot\text{cm}^{-1}$, T is absolute temperature in degree Kelvin, k_B is Boltzmann constant, and L is Lorentz number.

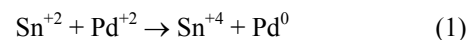
3. RESULTS AND DISCUSSION

3.1. Surface Treatment of Diamond Powders Surface Cleaning and Etching

The coating process of diamond powders is highly dependent on the pre-treatment of the powders themselves. The first pretreatment step is to remove any foreign matter may be existed from the reinforcement powders. Acetone was used to remove any organic matter, such as grease or oil, and finally used 50% HNO_3 for further cleaning the powder surfaces and also to etch their surfaces. This pretreatment increases the ability of diamond surface to be coated, increases the homogeneity of the coating film and improves the adhesion of coating layer. Although the coating bath is the most visible and complex, any process problem is almost not due to the chemistry of the bath itself, but is more likely due to the pre-treatment of the surface of the substrate.

Activation (Metallization) of Diamond Surfaces

The main purpose of the metallization process for diamond powders is to etch and provide active sites that can react with the activators as well as to convert the hydrophobic to hydrophilic surface. Adding sensitized powders to the activation bath, the tin ions that are adsorbed on the diamond surfaces, reduce the palladium ions in the activation step according to the following equation:



This step results in imparting a uniform surface film to the diamond powders, which ensures uniform adsorption of subsequent coating and therefore promotes better coating [16].

3.2. NiWB Electroless Plating

The coatings are deposited on the surface of diamond found in the solution once its pH value becomes 6.5 and its temperature 85°C . NiWB coating process used in this investigation is a chemical reduction process by dimethyl amine borane (DMAB) which served as a reducing agent to supply electrons for the reduction process. The diamond powders coated with NiWB are investigated by scanning electron microscope and the X-ray diffraction. The scanning electron micrograph of the diamond coated is shown in **Figure 1**. Continuous coating is seen on the surfaces of diamond. **Figure 2** illustrated the chemical composition and the obtained average data of the coated layer using EDS. It was interesting to note that the nickel content of the deposit is higher than the tungsten content, suggesting an anomalous behavior that involves a preferential deposition of electrochemically less noble in the deposit. Saito *et al.* [17] have also observed this anomaly and suggested that the low overvoltage for nickel deposition is the reason for its

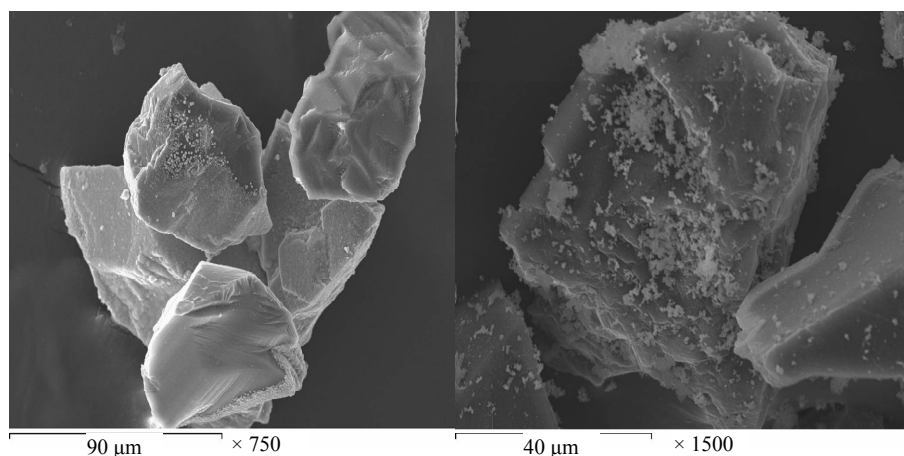


Figure 1. SEM image for the diamond coated with NiWB film.

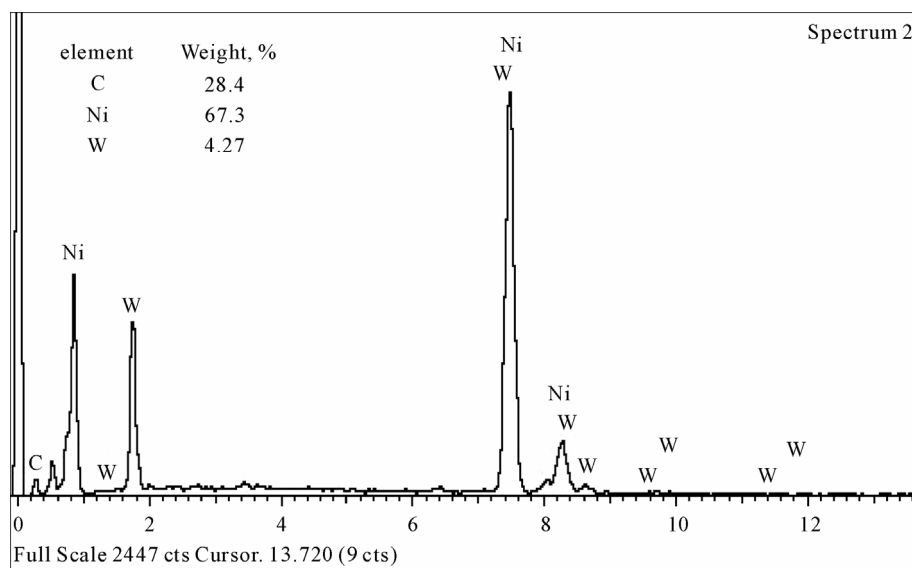
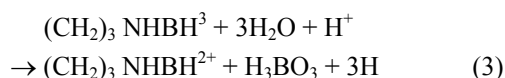
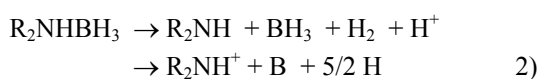


Figure 2. EDS analysis of the diamond coated with electroless NiWB.

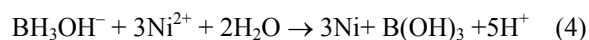
preferential deposition in the electroless deposit. The B content in the film was determined by inductively coupled plasma-mass spectrometer (ICP-MS). The analysis proved that the B content in the NiWB film was 5 wt%. View Within Article

XRD pattern for uncoated and coated diamond before and after heat treatment is illustrated in **Figure 3**. **Figure 3(a)** shows the peaks at 2θ of 440 and 750 which attributed to the pure diamond powder, while XRD pattern for diamond powder coated with NiWB as a deposit (**Figure 3(b)**) is seen the presence of sharp peak represent the presence of W at 35° and peaks represent the presence of diamond at 75° and broad peak with low intensity at 45° represent the deposition of Ni alloy in amorphous structure. When the coated powders after heat treatment under reducing atmosphere at 900°C for 1 hr were examined by XRD in order to find out any reaction, the pattern reveals that the amorphous coated converted to crystalline one. Crystallization induced by heating was confirmed by the appearance of diffraction lines corresponding to WB_2 at 2θ of 37° , BC_2 at 75.5° , Ni_3B at 45° and C at 41.5 , 51 , 54.5 and 60° as those indicated in **Figure 3(c)**.

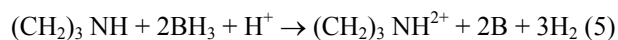
The mechanism of electroless NiB has been studied by many researchers [18,19]. Nevertheless, the mechanism of formation of NiWB remains unclear. In traditional NiB solution, the acid hydrolysis of DMAB occurs according to the following equations [17]:



Most authors believe that the major species supplying electrons for metal-ion reduction is BH_3OH^- . The hydrolysis investigation of DMAB shows that hydrolysis is pronounced at $\text{pH} < 5$. So, a significant amount of DMAB is wasted by the hydrolysis, and consequently the electroless deposition in this range should be avoided [20,21]. In the pH region above 5, the consumption of DMAB by hydrolysis approaches a minimum. Mallory proved that the rate of Ni deposition increases with an increase in DMAB for all investigated pH values within the range 6 to 11 [20]. However, it should be noted that an increase in pH within this range leads to a decrease in the rate of Ni deposition. This can be attributed to the increase in the solution stability (probably because of the tendency to hydrolyze at very high pH). Under these conditions, the reduction reaction may start in the bulk solution and the rate of deposition decreases. Consequently, the deposition efficiency decreases. Additionally, Mallory suggested that the preferred operating pH range for Ni deposition with DMAB is 6 to 7 (near neutral) [21]. Generally, DMAB has three active hydrogen atoms bonded to the boron, and theoretically should reduce three metal ions (such as Ni) for each ion of BH_3OH^- .



The boron reduction can be represented by the following reaction:



The tungsten deposition mechanism itself is not clear yet. There are some proposed models that explain the fact that tungsten cannot be deposited either electrochemically or chemically by itself, but it can be deposited

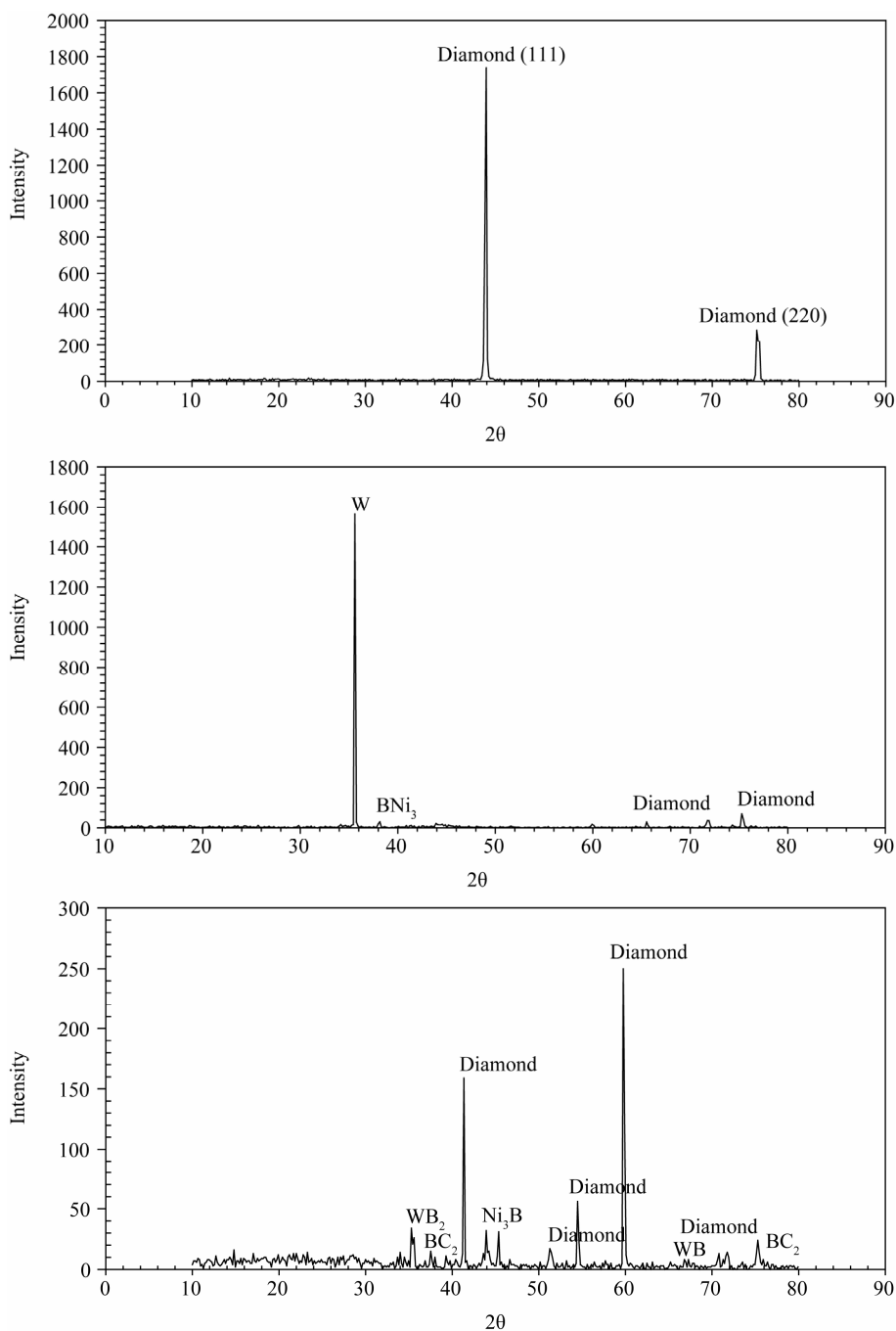
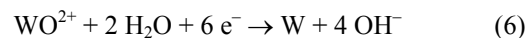


Figure 3. X-ray diffraction for diamond uncoated and coated with NiWB where, (a) diamond pure, (b) diamond coated before heat treated and (c) diamond coated after heat treatment at 900°C.

with iron group metals [22]. This mechanism should take into consideration the pH and that the metals are complexes with the citrate. In the simplest case, this ion should have the formula $[(\text{WO}_4)(\text{cit})]_{x-5}$ but this is, however, unstable. Several protonated forms of this complex are known, such as $[(\text{WO}_4)(\text{cit})(\text{H})_x]_{x-5}$, where x can assume values of 1 - 3. The reduction of these ions

can be presented as:



3.3. Composites Fabrication

Consolidation of metallic powders is mainly carried out using compaction followed by sintering. Sintering is

a thermal process which increases the strength of a powder mass by bonding adjacent particles via diffusion or related atomic level events. As a result of this operation, the material acquires the required physical and mechanical properties. Most of the properties of a powder compact are improved with sintering. All the prepared composites were investigated by the SEM, and exposed to different physical and mechanical tests.

In order to make clear the difference in wettability of un-coated and coated diamond with Cu matrix, the surface morphologies of the sintered materials with different volume fraction diamond mixed with copper were observed by SEM. **Figures 4(a)-(f)** illustrate the dispersion of uncoated or coated diamond particles in the copper matrix. One can notice that the distribution of uncoated diamond (**Figures 4(a)-(c)**) or coated diamond (**Figures 4(d)-(f)**) increases with increasing diamond $V_f\%$ in the composite. The Cu/coated diamond composite has low porosity than Cu/un-coated diamond composite. Additionally, the distribution of diamond in the composite made from Cu/coated diamond powders is more uniform with good wettability than those of the composite made from Cu/uncoated diamond powders. Since the uncoated diamond particles are easy to be stripped off during mechanical polishing, small pits are left on the surface of samples. While, the composite made from Cu/coated diamond powders has low porosity content due to less Cu-C contacts during sintering, and the metallic binders (coated film) decrease all the existing cavities between Cu particles. The uniform distribution and a maximum value of the diamond in the composite were observed at 20% V_f .

3.4. Characterizations of the Fabricated Composites

3.4.1. Densities Calculation

The density of the copper/diamond composite is one of the most important properties due to its effect on the other properties. It is very sensitive to composition and porosity in the sample and is widely used as a quality control test. The densities and relative densities of the sintered copper/diamond composite materials with different diamond $V_f\%$ are reported in **Table 3**. The relative density of the sintered materials was calculated according to the following formula:

$$\text{Relative density } (Rd\%) = (\delta_s / \delta_t)\% \quad (7)$$

where δ_s , and δ_t are the densities of sintered density (actual density) and theoretical density respectively.

The data reveals that the density of composite materials containing coated diamond with NiWB has higher value than that composite containing uncoated diamond

Table 3. The densities and relative densities percentage of the sintered materials with different $V_f\%$ of diamond.

Investigated composites	ρ_s	ρ_t	$Rd\%$
Cu/uncoated diamond with different $V_f\%$			
10	5.78	8.33	69.46
15	5.86	8.045	72.25
20	6.30	7.76	81.18
30	6.66	7.19	60.00
Cu/coated diamond with NiWB with different $V_f\%$			
10	6.27	8.33	88.6
15	6.08	8.04	82.29
20	5.50	7.76	99.7
30	4.50	7.19	92.6

particle. This is can be attributed to the excellent wettability between Cu matrix and coated diamond than in case of composite containing uncoated diamond due to high solubility of Ni in Cu. Coated film is used as a bonding matrix because its wetting or capillary action during solid phase sintering allows the achievement of high densities; this improvement could be attributed to the ability of B and W to form carbide phases as shown in XRD analysis (**Figure 3**). XRD pattern can't prove the formation of tungsten carbide phase owing to low concentration of W compared to the concentration of Ni in the coated layer or carbon of the substrate. This results agreement with Q. Sun [9] who proved that pure liquid copper does not wet diamond, while well in presence of carbide which promotes wetting and bonding of diamond.

3.4.2. Hardness Measurements

Hardness measurements were used to investigate the strengthening effect of diamond particles as a reinforcement material and to distinguish the surface imperfection. **Table 4** illustrates the hardness of the investigated composite materials. As can be seen, hardness of sintered materials made from coated diamond is higher than those made of uncoated diamond powders. Also hardness increases with increasing $V_f\%$ of diamond powder in the matrix. It is evident that Cu-20 $V_f\%$ coated diamond composites have the highest hardness values of all investigated composites, not only because of the strengthening effect of diamond but also due to the high density and low porosity content. While, in the case of the uncoated diamond, there is no any adhesion

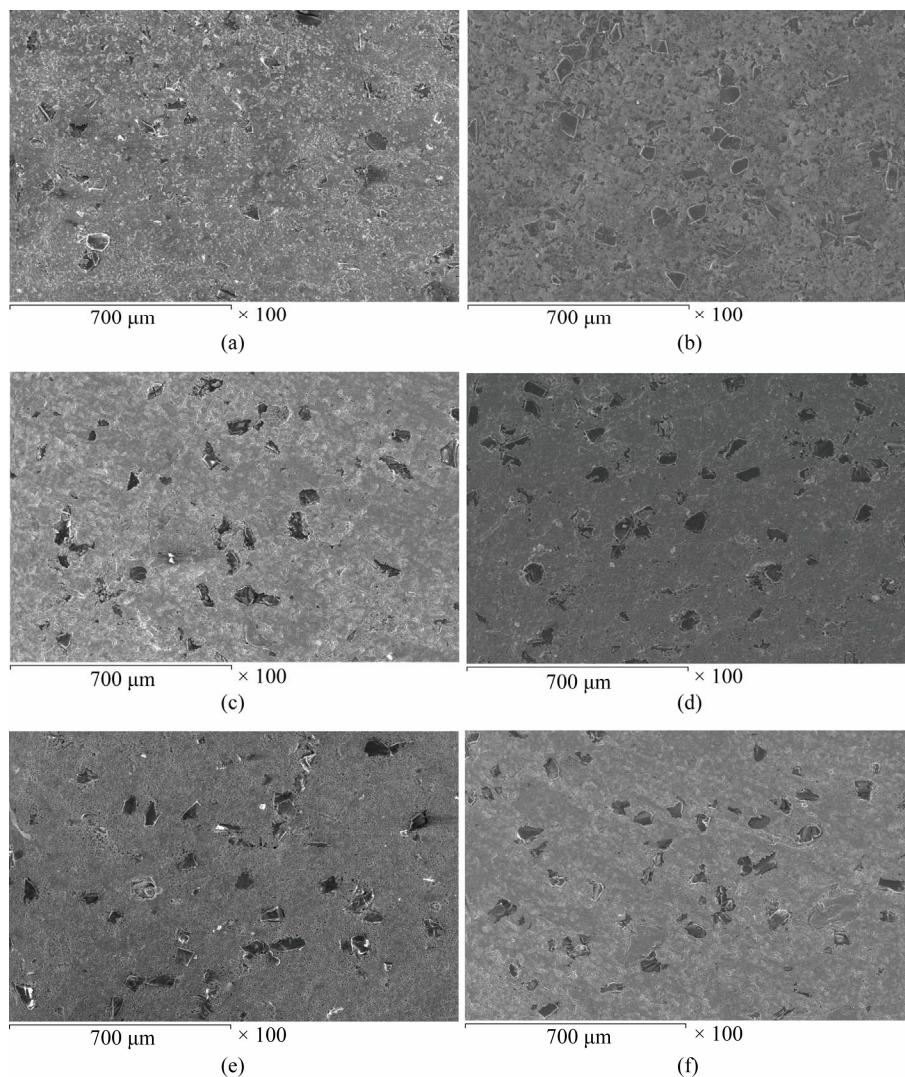


Figure 4. Surface morphologies of the as-polished Cu/uncoated diamond and Cu/NiWB coated diamond composites prepared by PM technique containing different $V_f\%$ diamond where: (a)-(c) Cu/10, 20, 30 $V_f\%$ uncoated diamond respectively and (d)-(f) Cu-10, 20, 30 $V_f\%$ NiWB coated diamond.

or bond between the diamond and the copper matrix which causes the formation of pores in the final composite and hence showed low hardness.

3.4.3. Electrical Conductivity Measurements

The electro friction materials that exposed to high current densities or high voltages are produced from a composite material that having high electrical and thermal conductivities. Copper/diamond composite has a good sliding, antifriction properties, and high electrical and thermal conductivity [23]. The measured resistivity was converted to electrical conductivity IACS% (International Annealed Copper Standard) according to the ASTM standard B 193-72.

The results of electrical resistivity measurements of

the fabricated composites are shown in **Table 5**. It can be noticed that the electrical resistivity for all investigated Cu/diamond composites decreases with increasing $V_f\%$ of diamond up to 20 $V_f\%$ and then slightly increase. At the same time, the electrical resistivity for the composite fabricated from coated diamond with NiWB is lower than that of composite fabricated from uncoated diamond. This can be rationalized by the high porosity of the Cu/uncoated diamond composite. This porosity was resulted from the weak bond between diamond and the Cu matrix as shown in **Figure 4**. This in turn, creates voids, which decreases the mobility of the free electron causing high resistivity [24,25]. The electrical conductivity is directly affected by porosity, the greater the void content the lower is the electrical conductivity. While, in

Table 4. The Vicker Macro-Hardness values of the investigated composites.

Investigate Composites	Hardness Values, HV
Pure copper	52.00
Cu/uncoated diamond	
Cu/10 V% uncoated diamond	55.00
Cu/15 V% uncoated diamond	55.00
Cu/20 V% uncoated diamond	56.00
Cu/30 V% uncoated diamond	52.00
Cu/coated diamond with NiWB	
Cu/10 V% coated diamond	66.35
Cu/15 V% coated diamond	77.04
Cu/20 V% coated diamond	87.45
Cu/30 V% coated diamond	74.24

Table 5. The electrical resistivity of the investigated composites.

Investigate Composites	electrical resistivity	
	Resistivity ($\mu \cdot \text{cm}$)	IACS%
Pure copper chemically deposited	2.1	82.00
Cu/uncoated diamond		
Cu/10 V% uncoated diamond	2.33	74.00
Cu/15 V% uncoated diamond	2.085	82.5
Cu/20 V% uncoated diamond	1.96	87.75
Cu/30 V% uncoated diamond	2.00	86.00
Cu/coated diamond with NiWB		
Cu/10 V% coated diamond	1.78	97.00
Cu/15 V% coated diamond	1.74	99.00
Cu/20 V% coated diamond	1.73	99.40
Cu/30 V% coated diamond	1.75	98.30

case of Cu/coated diamond composites the pores is low due to the presence of a metallic bond between the coated layer on the diamond surface and the copper matrix. The NiWB coated diamond composite has the highest and more conductive sample due to the following reasons:

- The highest density and lowest porosity of the materials.
- The good adhesion force between the carbide coating with diamond surface on one side and the copper matrix on the other side.
- The presence of a carrier layer at the interface be-

tween the copper matrix and the diamond, which transfer the high electrical conductivity properties of the copper to the diamond.

- The high hardness of carbide layers which increase the effect of compaction pressure on Cu-matrix on one side and protect diamond from fragmentation on the other side.

3.4.4. Transverse Rupture Strength (TRS)

Transverse rupture strength (TRS) is the most common method for determining the fracture strength of composite materials; it is the maximum stress that is encountered during a three-point bending test. In the same time the TRS testing method is more suitable than the tensile measurement for determining the strength of materials processed by powder metallurgy. There are several reasons for its popularity in practice. First of all, TRS is very sensitive to porosity levels. When porosity level is high, TRS values will be not only poor but also very inconsistent. Therefore, it has historically being used as an indicator of the quality of sintered composite materials in manufacturing. Secondly, because of its sensitivity to pores and other defects, TRS is often also viewed as a measure of "toughness".

The effect of diamond $V_f\%$ (10^{-30}) in the Cu matrix on the TRS was studied and the values were listed in **Table 6**. According to the data obtained, the TRS increases with increasing the diamond $V_f\%$ in the Cu matrix and attains the optimum values at 20%.

One can notice that the TRS of the Cu/coated diamond composites are much higher than those made from Cu/uncoated diamond composites. This can be explained by the fact that, the coated layer which consists of carbides and borides acts as crack propagation layer that transfer the strength of diamond to the copper matrix and

Table 6. The TRS values for the investigated composites.

Investigate Composites	TRS Values, N/mm ²
Cu/uncoated diamond	
Cu/10 V% uncoated diamond	210.00
Cu/15 V% uncoated diamond	238.00
Cu/20 V% uncoated diamond	250.00
Cu/30 V% uncoated diamond	270.00
Cu/coated diamond with NiWB	
Cu/10 V% coated diamond	438.65
Cu/15 V% coated diamond	753.37
Cu/20 V% coated diamond	755.00
Cu/30 V% coated diamond	652.60

also permit a good adhesion between the diamond and the copper matrix that gives more density and less porosity, consequently more strengthened composite. But in case of the uncoated diamond composite, there is no real bonding between diamond and copper matrix, so the adhesion force is very weak, which creates space bonding that deteriorate the strength of the composite.

But if we view the fracture process during TRS testing as consisting of crack initiation and propagation processes and assume the ideal case when the effects of porosity is negligible, the crack initiation process will dominate when the hardness is high and the fracture toughness is very low. Therefore the higher the hardness is, the higher the stress that is needed for crack initiation and hence the higher the TRS. This means that, the TRS of the investigated Cu/coated diamond is much greater than the Cu/uncoated diamond. The explanation of the

result is as follows; in Cu/coated diamond the crack resistance is greatest in the coating film, followed by the Cu grains and the Cu/diamond interface. The coating grains act to impede rapid crack growth and absorb more energy than the uncoated diamond, thus increasing the fracture toughness of the material.

The fracture micrographs of the investigated materials are shown in **Figure 5**. **Figures 5(a)** and **(b)** indicate the fracture surface of the Cu/uncoated diamond composite at low and high magnification respectively. **Figure 5(b)** illustrates poor bonding on (111) diamond surfaces with Cu matrix as shown in XRD analysis. Marked A in **Figure 5(b)** indicates regions where the Cu matrix has adhered to diamond surfaces. This adhesion between Cu and diamond was consistently observed on (220) diamond faces as described by P. W. Ruch *et al.* [6]. **Figures 5(c)** and **(d)** show the fracture surface of the Cu/

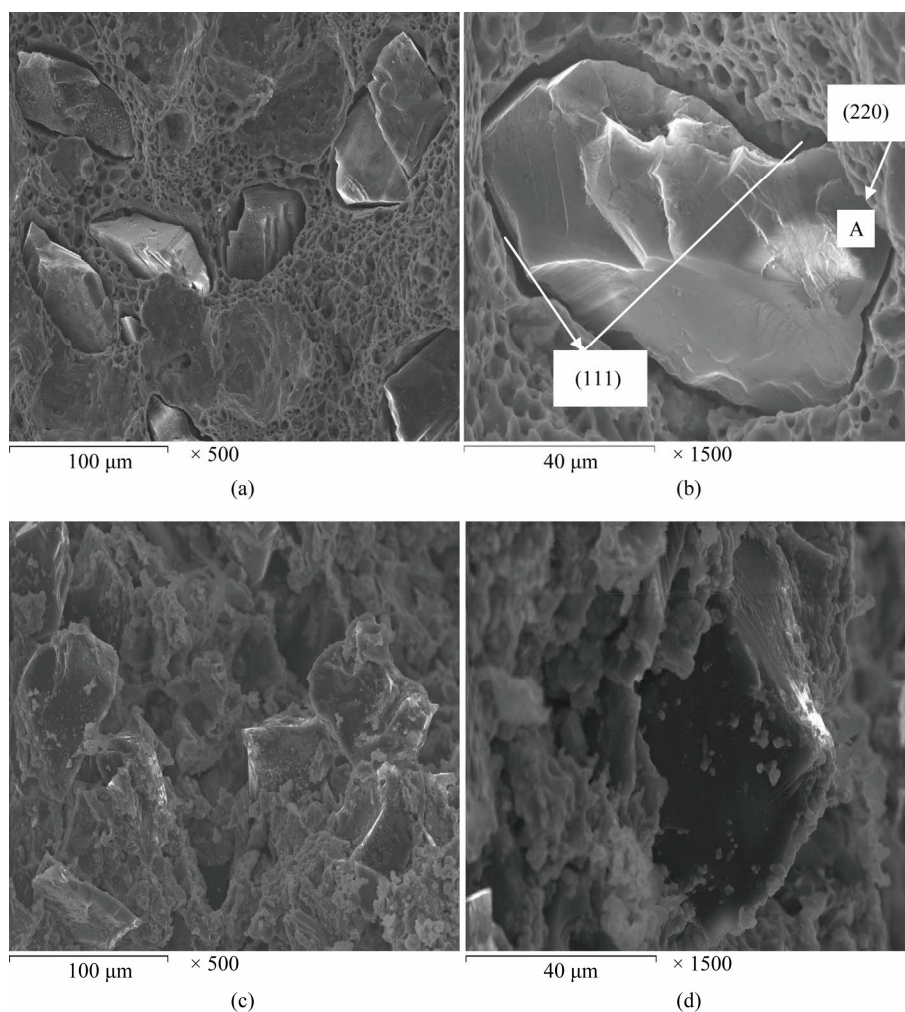


Figure 5. SEM micrograph of the fracture surface of Cu/uncoated and coated diamond composite, where (a) Cu/uncoated diamond at low magnification, (b) at high magnification, (c) Cu/NiWB coated diamond composite at low magnification, and (d) Cu/NiWB coated diamond composite at high magnification.

NiWB coated diamond composite at low and high magnification respectively. **Figure 5(d)** illustrates the improving in the adhesion force between coated diamond surface and Cu matrix. NiWB coated diamond acts as a filler continuous layer that decreases the pores at the interface and so gives a degree of adhesion that increases the strength of the final composite.

3.4.5. Thermal Conductivity and CTE of Investigated Composites

Table 7 shows the variation of thermal conductivity and CTE of pure Cu and different composites with optimum $V_f\%$ diamond (20% V_f). It is clear that thermal conductivity increased from 378 for Cu/uncoated diamond composite to 430 W/mk for Cu/coated diamond composites. This means that coated diamond improved the thermal conductivity of the Cu/diamond composite. Adding uncoated diamond particles to Cu matrix caused slight increase (378 W/mK) in the thermal conductivity of pure Cu. The low thermal conductivity of this composite was indicating a high thermal barrier resistance. This result due to separation between copper and diamond, *i.e.* diamond particles are surrounded by cavities, which lead to low chemical affinity between copper and diamond. Therefore, it is difficult to produce a bond of low thermal resistance and high mechanical strength between the matrix and the reinforcement. While adding NiWB coated diamonds lead to increase the thermal conductivity of the composites, which demonstrated the effectiveness of the coated layer to obtain a good thermal contact between the matrix and the diamond particles.

Thermal expansion coefficient of copper/diamond composites, namely, Cu/20 $V_f\%$ uncoated diamond and Cu/20 $V_f\%$ coated diamond was measured. It can be seen that the CTE of Cu/coated diamond decreases to $6 \times 10^{-6} \text{ K}^{-1}$, which is about one-third of that of the pure copper (17×10^{-6}). The lower CTE of Cu/coated diamond composite is related to the good bonding between the metal matrix and the diamond particle. This indicates that NiWB coated diamond are a promising reinforcement to lower the CTE of heat sink materials.

4. CONCLUSIONS

1) Diamond powders can be coated with NiWB alloy by electroless technique.

2) The sintered materials made from coated powders exhibit better structure homogeneity, higher densification, electrical resistivity, hardness and TRS properties than those made from mixed powders.

3) This work demonstrates that high thermal conductivities can be achieved for Cu/coated diamond compos-

Table 7. Thermal conductivity and CTE of the investigated composites.

Investigate Composites	Thermal conductivity, (W/mk)	CTE, $10^{-6}/\text{k}$
Pure copper	352	17
Cu/20 $V_f\%$ uncoated diamond	378	10
Cu/ 20 $V_f\%$ coated diamond	430	6

ite. The formation of a carbide and boride layer is crucial to enable the manufacturing of Cu/diamond heat sinks with high thermal conductivities up to about 430 W/mK combined with CTE of $6 \times 10^{-6}/\text{K}$.

4) Further work address some critical characteristics of composites, in order to promote a better coupling of matrix and reinforcement, thus leading to improved physical and mechanical characteristics.

REFERENCES

- [1] Ellsworth, M.J. (2004) Chip power density and module cool technology projections for the current decade. *Proceedings of the 9th Intersociety Conference on Thermal and Thermo Mechanical Phenomena in Electronic Systems*, Las Vegas, **2**, 707-708.
- [2] Zweben, C. (1998) Advances in composite materials for thermal management in electronic packaging. *Journal of Management*, **50**, 47-51.
- [3] Zweben, C. (2001) Thermal management and electronic packaging applications. *ASM Handbook*, **21**, 1078-1084.
- [4] German, R.M., Hens, K.F. and Johnson, J.L. (1994) Powder metallurgy processing of thermal management materials for microelectronic applications. *International Journal of Powder Metallurgy*, **30**, 205-215.
- [5] Evans, T.C. (1998) Thermal properties of electronic materials. *Thermal Management Handbook for Electronic Assemblies*, McGraw-Hill, New York.
- [6] Ruch, P.W., Beffort, O., Kleiner, S., Weber, L. and Ugowitzter, P.J. (2006) Selective interfacial bonding in Al(Si)-diamond composites and its effect on thermal conductivity. *Composites Science and Technology*, **66**, 2677-2685. doi:10.1016/j.compscitech.2006.03.016
- [7] Clyne T.W. (2000) Thermal and electrical conduction in MMCs. In: Kelly, A., Chou, T.W., Talreja, R., Clyne, T.W., Warren, R., Carlsson, L., *et al.*, Eds., *Comprehensive Composite Materials. Metal-Matrix Composites*, Elsevier, Amsterdam, **3**.
- [8] Weber, L. and Tavangar, R. (2007) On the Influence of active element content on the thermal conductivity and thermal expansion of Cu-X (X = Cr, B) diamond composites. *Journal of Materials Science*, **57**, 988-991.
- [9] Schubert, T., Ciupinski, L., Zielinski, W., Michalski, A., Weigärber, T. and Kieback, B. (2008) Interfacial characterization of Cu/diamond composites prepared by powder metallurgy for heat sink application. *Scripta Materialia*, **58**, 263-266. doi:10.1016/j.scriptamat.2007.10.011
- [10] Schubert, T.H., Ciupiński, L., Morgiel, J., Weidmüller, H., Weissgärber, T. and Kieback, B. (2007) Advanced com-

- posite materials for heat sink applications. *Euro PM 2007—PM Functional Materials*, Toulouse, 15-17 October 2007.
- [11] Lowenheim, F.A. (1974) Modern electroplating. John Wiley and Sons, New York.
- [12] Metal Powder Industries Federation, Princeton (1998).
- [13] Fang, Z. and Eason, J.W., (1993) Nondestructive evaluation of WC-Co composites using magnetic properties. *International Journal of Powder Metallurgy*, **29**, 259-265.
- [14] Deborah, C.D.L. (2001) Applied materials science application of engineering materials in structural, electronics, thermal and other industries. Chapman and Hall, London.
- [15] Moustafa, S.F., Abdel, H.Z., Osama, B.G and Hussien, A. Synthesis of WC hard materials using coated powders. *Advanced Powder Metall*, **22**, 596-601.
- [16] Saito, T., Sato, E., Matsuoka, M. and Iwakura, C.J., (1998) Electroless deposition of Ni-B, Co-B and N-Co-B alloys using dimethyl amineborane as a reducing agent. *Applied Electrochemistry*, **28**, 559-563. [doi:10.1023/A:1003233715362](https://doi.org/10.1023/A:1003233715362)
- [17] Osaka ,T. Takano, N., Kurokawa, T., Kaneko, T. and Ueno, K. (2003) Characterization of chemically-deposited NiB and NiWB thin films as a capping layer for ULSI application. *Surface and Coatings Technology*, **169-170**, 124-127. [doi:10.1016/S0257-8972\(03\)00186-5](https://doi.org/10.1016/S0257-8972(03)00186-5)
- [18] Duhin, A., Sverdlov, Y., Feldman, Y. and Shacham-Diamand, Y. (2009) Electroless deposition of NiWB alloy on p-type Si(100) for NiSi contact metallization. *Electrochimica Acta*, **54**, 6036-6041. [doi:10.1016/j.electacta.2009.01.062](https://doi.org/10.1016/j.electacta.2009.01.062)
- [19] Mallory, G.O. (1971) The electroless nickel plating bath: effect of variables on the process. *Plating*, **58**, 319-322.
- [20] Mallory, G.O. and Hadju, J.B. (1991) Electroless plating: Fundamentals and applications. AESF, Orlando.
- [21] Abdel, A.A., Barakat, H., Abdel, H.Z. (2008) Synthesis and characterization of electroless deposited Co-W-P thin films as diffusion barrier layer. *Surface & Coatings Technology*, **202**, 4591-4597. [doi:10.1016/j.surfcoat.2008.03.023](https://doi.org/10.1016/j.surfcoat.2008.03.023)
- [22] Pearlstein, F. and Weightman, R.F. (1974) Electroless cobalt deposition from acid baths. *Journal of The Electrochemical Society*, **121**, 1023-1028. doi.org/10.1149/1.2401971
- [23] Ellis, D.L. and McDanel, D.L. (1993) Thermal Conductivity and thermal expansion of graphite fiber-reinforced copper matrix composites. *Metallurgical and Materials Transactions A*, **24**, 43-52. [doi:10.1007/BF02669601](https://doi.org/10.1007/BF02669601)
- [24] Abdel, G. and El-Kad, O. (2005) Improvement of wettability of carbon fiber by in-situ carbide coating. Ph.D. Thesis, Cairo University, Cairo.
- [25] Khattab, N.M.M. (2001) Ph.D. Thesis, Department of Chemistry, Faculty of Girls, Ain Shams University, Cairo.